

# Edge Stability and Boundary Shaping in Tokamaks

S.Yu.Medvedev<sup>1</sup>, A.A.Ivanov<sup>1</sup>, A.A.Martynov<sup>1</sup>, Yu.Yu.Poshekhonov<sup>1</sup>,

S.H.Kim<sup>2</sup>, J.B.Lister<sup>2</sup>, Y.R.Martin<sup>2</sup>, O.Sauter<sup>2</sup>, L.Villard<sup>2</sup>

<sup>1</sup>*Keldysh Institute, Russian Academy of Sciences, Moscow, Russia*

<sup>2</sup>*CRPP, Association Euratom-Confédération Suisse, EPFL, Lausanne, Switzerland*

Edge stability calculations performed with the KINX code showed that local curvature perturbations, especially at the LFS of the plasma boundary, can control the second stability access and change the edge kink/ballooning mode stability boundaries and the most unstable mode toroidal wave numbers, potentially leading to different ELM regimes [1].

Calculations of the edge stability diagrams for the reconstructed equilibria from the recent TCV shots with applied plasma boundary deformation shows several percent difference in the stability limits for the equilibria before and after the perturbation. Such a difference would be certainly perceptible in type-I ELM triggering/pacing experiments but most probably not during the slow evolution of the magnetic configuration. The qualitative changes in the ELM behavior (ELM type-I to type-II transition) can be expected in the large ELM regime with additional heating when the second stability access is eliminated due to the plasma boundary shaping. For that purpose several shapes of the TCV plasma boundary have been considered taking into account the constraints on the PFC system.

The quasi-equilibrium modeling of the ASDEX-UG ELM pacing experiment with different patterns of the plasma movement [4] shows that the plasma boundary perturbations and the corresponding changes in the stability boundaries are consistent with the triggered ELM behavior in the experiment.

The problem of optimal plasma shaping for ELM control based on ideal MHD stability calculations for ITER plasma, taking into account the separatrix at the plasma boundary, is considered.

## 1 TCV edge stability with local boundary shape perturbations

The pedestal profiles for the shot #26383 [2] and plasma boundaries for the shot #32696 at times  $t=0.6$  and  $t=1.0$  (before and during the application of the boundary perturbation) were used to generate the basic equilibria for stability studies. The effect of the boundary perturbation on the local shear is demonstrated in Figure 1. The stability diagrams (Figure 2) were obtained by independently rescaling the parallel current density and pressure gradient in the pedestal.

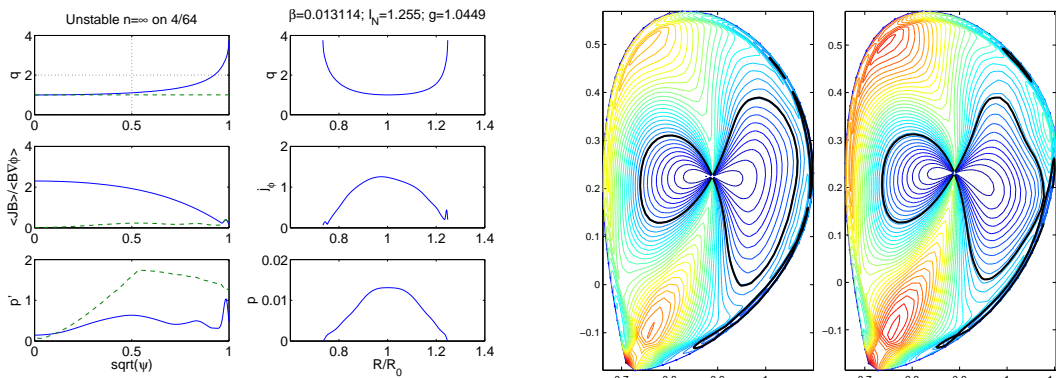


Figure 1. The plasma profiles based upon the reconstructed electron temperature and density profiles for the TCV shot #26383 and local shear distribution (zero shear - bold black) for the shot #32696  $t = 0.6$  (left) and  $t = 1.0$  (right).

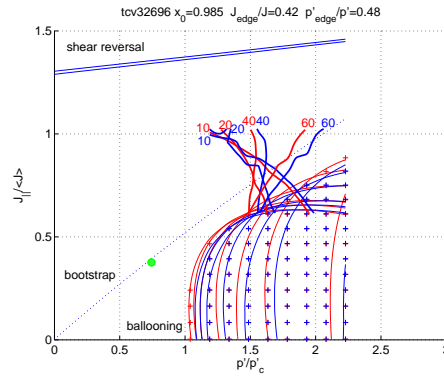


Figure 2. The edge stability diagrams for the two time moments ( $t = 0.6$  - blue colour;  $t = 1.0$  - red colour) for the TCV shot #32696. The crosses and thin lines show the high- $n$  ballooning mode stability boundaries (overall through the whole pedestal and for individual magnetic surfaces respectively). Bold lines give the stability boundaries for edge kink/ballooning modes (toroidal wave numbers are shown). The green circle show the pedestal parameters for the basic equilibrium with the profiles from Figure 1.

The equilibrium reconstructed with the LIUQE code for the TCV shot #32696 was reproduced with the free boundary equilibrium code SPIDER [3]. Taking the reconstructed boundary as the contour in the  $(R, Z)$  plane to be fitted in the inverse equilibrium problem, three different perturbations were applied by introducing additional control points, through which the modified plasma boundary passes. The boundaries for the three cases marked as "xo" (large curvature on the outboard side), "xx" (increased squareness in the up-down symmetric manner) and "x" (large perturbation due to the outboard x-point proximity) are compared to the reconstructed TCV plasma boundaries in Figure 3.

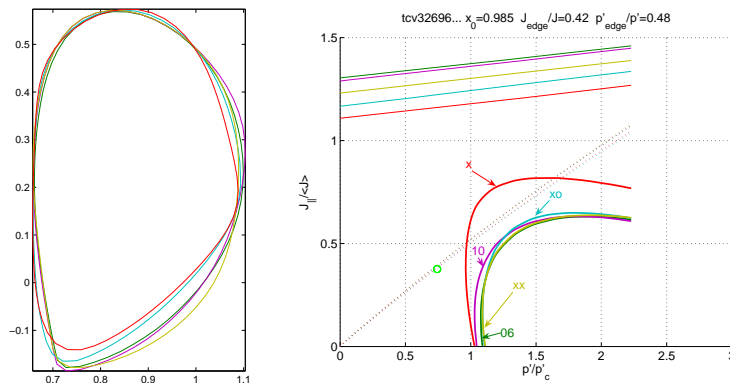


Figure 3. The plasma boundaries for the TCV shot #32696 ( $t=0.6$  - green,  $t=1.0$  - magenta) and the three other perturbations ("xo" - cyan, "xx" - yellow, "x" - red) (left) and the corresponding high- $n$  stability limits at the top of the pedestal (right).

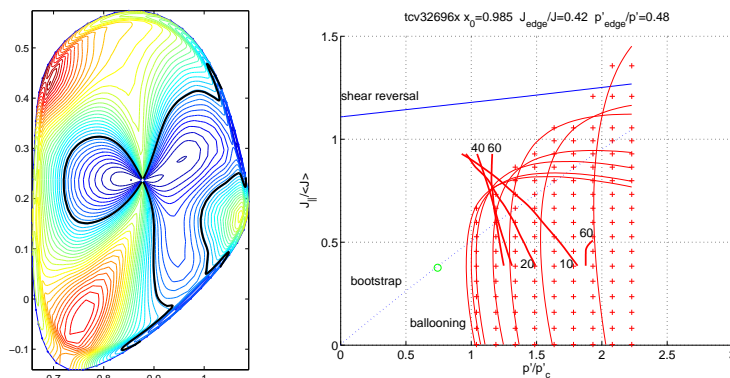


Figure 4. The local shear level lines (left) and edge stability diagrams for the TCV boundary perturbation due to the outboard x-point proximity ("x") (right).

The complete edge stability diagram for the case "x" is shown in Figure 4. The proximity of the x-point to the plasma boundary at the outboard side results in lower pressure gradient limits against medium-n modes and the second stability access for the high-n mode taking place only for large current density (higher than the bootstrap current density) in the pedestal. The latter feature may be related to the change in the ELM type.

## 2 ELM pacing in ASDEX with different patterns of the plasma motion

ELM triggering by fast plasma motions in the vertical direction (z wobbling) was found to be successful both at TCV and ASDEX-Upgrade tokamaks. Modeling using the DINA-CH code indicated that radial wobbling could produce similar results since the expected deformation at the plasma edge and the induced edge current pattern can reach similar strength [4]. However, radial wobbling performed at the same amplitude as successful vertical wobbling did not result in ELM triggering [5].

The systematic study of the plasma boundary perturbations due to different patterns of plasma motion was performed using the DINA-CH/SPIDER quasi-equilibrium simulation taking into account the magnetic field diffusion. The profiles for the initial equilibrium were chosen the same as in [6] being close to the edge kink/ballooning stability boundary considered as ELM type I trigger. The comparison of the plasma boundary curvature perturbation patterns shows that the inward radial plasma motion corresponds to the plasma curvature increase in the upper part of the plasma boundary accompanied by its decrease in the lower part (Figure 5). That is in contrast to the downward plasma motion when the curvature increased simultaneously above and below plasma equatorial plane at the low field side. It leads to small but systematic differences in the stability margin behavior.

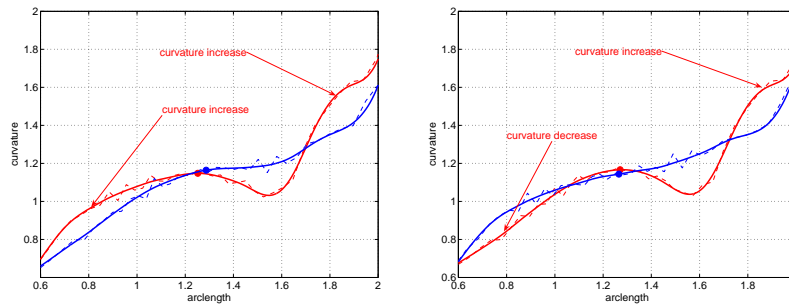


Figure 5. The plasma boundary curvature perturbations versus the plasma cross-section arclength for the ASDEX ELM triggering model. The positions of the outermost points are marked by circles. Vertical (left) and radial (right) wobbling. The downward/inward (red) and upward/outward (blue) directions of motion.

## 3 ITER upper plasma shaping

The sensitivity study of the edge stability to the top plasma shaping in ITER was performed using series of equilibria calculated with the SPIDER code. The initial equilibrium corresponds to the Scenario 2 plasma with the fitting and control points at the plasma boundary prescribed according to the conventional separatrix shape and x-point location. Increasing the z-coordinate of one of the control points near the plasma top makes the plasma shape change and eventually transform into a configuration close to double-null.

The changes in the edge stability between the single null and double null cases are presented in Figure 6. The parallel current density is very low at the separatrix for the conventional Scenario 2 profiles while the pressure gradient peaks to the edge. It results in the very plasma edge being in the first stability region of high-n ballooning modes. The decrease in the squareness in the upper part of the plasma for the double null configuration leads to lower current density needed for the second stability access in the pedestal (except for the very edge). It is accompanied by a significant shift of the stability margins for the medium-n modes. The eigenfunction structure doesn't change much. Another remarkable feature of the double-null configuration is the higher current density limit for the current driven modes in contrast to the analysis from [7].

For a finite current density at the plasma separatrix a similar stability behavior as in Figure 6 is obtained; the only difference is the current density limit of low  $n$  modes decreasing below that needed for shear reversal.

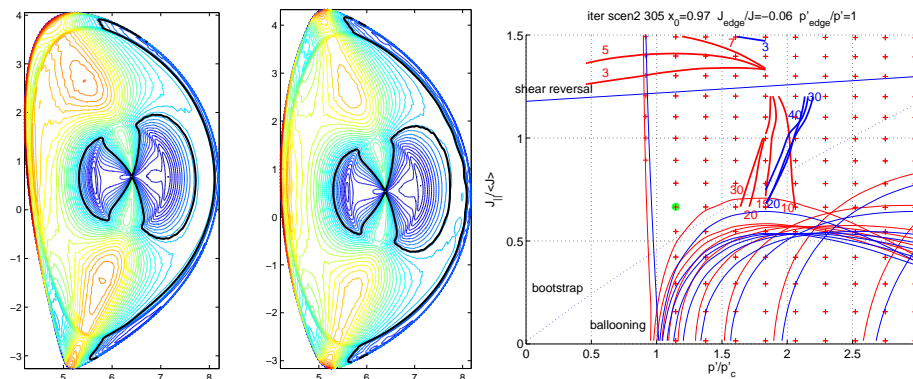


Figure 6. The local shear level lines and the edge stability diagrams for the conventional Scenario 2 ITER boundary (red lines) and double null configuration (blue lines).

#### 4 Conclusions

Several percent change in the edge stability limits due to the boundary perturbations in the TCV shot #32696 do take place: it is about 5% between the  $t=0.6$  and  $t=1.0$  for the shot #32696 (Figure 3). Such a change would be certainly perceptible in type-I ELM triggering/pacing experiments but then high frequency coils should be employed. Some qualitative changes in the ELM behavior (type-I to type-II transition) can be expected when the second stability access is eliminated (similar to the case "x"). The remarkable feature of the edge stability is the shift of the most unstable toroidal wave number to higher toroidal wave numbers accompanying higher current density needed for the second stability access.

The difference in the edge stability properties between the vertical and radial wobbling sequences was found related to the different patterns of the plasma boundary curvature perturbations at the LFS. Despite very similar perturbation levels for both cases, the curvature increase in the upper part of the plasma boundary accompanied by its decrease in the lower part during inward plasma motion leads to weaker changes in the edge stability limits. That is in contrast to the downward plasma motion, when the curvature increased simultaneously above and below plasma equatorial plane. The studied combined vertical/radial wobbling scenario doesn't provide significant changes in the edge stability compared to the radial wobbling case.

The proximity of the ITER plasma shape to a double null configuration was found beneficial to the current driven edge kink mode stability. Together with the lower squareness it results in better second stability access and larger pedestal pressure gradient limits. However no significant changes in the eigenfunction structure were discovered. Further analysis is needed to determine the possible causes of transition into small ELM regimes (type-II/grassy/type-V): quasi-double null configurations, high triangularity, high beta poloidal values or changes in the pedestal profiles.

- [1] S.Yu.Medvedev *et al.* 33rd EPS Conference on Plasma Phys. Rome, 19 - 23 June 2006 ECA Vol.30I, P-1.146 (2006)
- [2] R.Behn *et al.* Edge profiles of electron temperature and density during ELMy H-mode in ohmically heated TCV plasmas. Accepted for publication in Plasma Phys. Control. Fusion (2007)
- [3] A.A.Ivanov *et al.* 32nd EPS Conf. on Plasma Phys., ECA Vol.29C, P-5.063 (2005)
- [4] S.H.Kim *et al.* 32nd EPS Conference on Plasma Phys. Tarragona, 27 June - 1 July 2005 ECA Vol.29C, P-5.014 (2005)
- [5] P.T.Lang *et al.* Czech. J. Phys. **56** (2006) 1329
- [6] S.Yu.Medvedev *et al.* Magnetic ELM Triggering and Edge Stability of Tokamak Plasma. 32nd EPS Conference on Plasma Phys. ECA Vol.29C, P-5.064 (2005)
- [7] N. Aiba *et al.* Nucl. Fusion **47** (2007) 297

**Acknowledgements** The CRPP authors are supported in part by the Swiss National Science Foundation.